Ligand Binding and Slow Structural Changes in Chlorocruorin from *Spirographis spallanzanii*†

Andrea Bellelli,* Eugenio Lendaro, Rodolfo Ippoliti, Rebecca Regan,‡ Quentin H. Gibson,‡ and Maurizio Brunori

Department of Biochemical Sciences "Alessandro Rossi Fanelli" and CNR Center of Molecular Biology, University of Rome "La Sapienza", P. Aldo Moro 5, 00185 Roma, Italy, and Department of Biochemistry, Molecular and Cellular Biology, Cornell University, Ithaca, New York 14853

Received December 23, 1992; Revised Manuscript Received April 7, 1993

ABSTRACT: Chlorocruorin is a cooperative respiratory pigment found in the blood of polychaete worms; its prosthetic group is a derivative of the iron protoporphyrin IX, in which the vinyl group at position 2 is substituted by a formyl group. The quaternary structure of chlorocruorins is complex: myoglobin-like subunits are grouped in tetramers and tetramers in dodecamers; 12 dodecamers are assembled in the 3500-kDa particle. Chlorocruorin from *Spirographis spallanzanii* displays the following overall functional properties: (i) the oxygen affinity is lower than in human hemoglobin, while that of CO is similar if not higher; (ii) the rates of combination with oxygen and carbon monoxide are low; and (iii) the off rate of oxygen is comparable to that of human hemoglobin, while the off rate of CO is 10 times smaller. When CO is partially photolyzed with a long and powerful light flash (70 μs), rebinding is biphasic as in mammalian hemoglobins; however, the slowest rate is faster than that observed by stopped flow, suggesting that the unliganded protein decays from the liganded high affinity state (R) to an intermediate state before reaching the low affinity (T) state. Oxygen binding was followed by stopped-flow and flash photolysis. While partial photolysis yields a fast, second-order time course, stopped-flow experiments yield slow, biphasic, and non-second-order time courses. This pattern of reactivity was attributed to a slow conformational transition(s) which is (are) rare limiting with oxygen, but not with CO. Photolysis with a short (9-ns) laser pulse shows first-order rebinding processes, attributed (by analogy to hemoglobins) to the recombination of the ligand from inside the protein matrix (geminate rebinding). In the bimolecular processes observed by laser photolysis, the rebinding rate characteristic of the intermediate state is not observed; this was attributed to the relatively slow decay from the R to the intermediate state (X). These experiments indicate that (some of) the allosteric transition(s) in *Spirographis* chlorocruorin is (are) slow and populate(s) long-lived intermediates with reactivities different from those of the T and R states.

INTRODUCTION

Chlorocruorin (Chl[1]), a respiratory pigment from the blood of some polychaete worms, is a giant hemoprotein (M_r = 3500 KDa) which binds oxygen with high cooperativity, the maximum Hill coefficient being as high as n = 6 (Antonini et al., 1962a).

In contrast to hemoglobin and erythrocruorin, Chl is green, because its heme group is different with a formyl group at position 2 of the porphyrin macrocycle (where protoporphyrin IX has a vinyl group). The assembly of Chl and of the closely related erythrocruorins involves interactions between myoglobin-like oxygen binding subunits with M_r = 17 kDa and the so-called *linker chains* with M_r = 30 kDa; 12 hexadecamers or dodecamers, which contain only the oxygen-binding subunits, are linked together by the linker chains in the superimposed hexagonal layers observed in disk shaped particles by electron microscopy (Guerritore et al., 1965; Qabar et al., 1991). The presence of the linker chains lowers the iron content of chlorocruorins and erythrocruorins relative to that of hemoglobins and myoglobins (0.25% vs 0.33%); in fact, the iron content of *Spirographis spallanzanii* Chl is the lowest yet reported [0.16%, according to Antonini et al. (1962b)].

The minimum cooperative unit for oxygen binding is considerably smaller than the whole, disk shaped macromolecule: analysis of the oxygen binding curves suggests that only 6–12 sites are coupled by heme–heme cooperative interactions (Guerritore et al., 1965; Colosimo et al., 1974; Imai et al., 1985), whereas the structural data point to a cooperative unit containing either 16 (Suzuki & Gotoh, 1986; Fushitani & Riggs, 1988) or more probably 12 oxygen binding sites (Qabar et al., 1991; Vinogradov et al., 1991). The purified and partially characterized dodecameric subunits of Chl from *Eudistylia vancouverii* (Qabar et al., 1991; Gibson et al., 1992) were shown to be cooperative (from the kinetics of combination with carbon monoxide); moreover, it was possible to split them into three tetramers, which bind oxygen and CO reversibly. Thus, the architecture of this giant respiratory protein is hierarchically organized into oligomers of increasing complexity.

Interestingly, a hierarchical organization of the heme–heme interactions and their effects had already been proposed, with the concept of "nesting" of the allosteric interactions (Wyman, 1972; Robert et al., 1987) to account for cooperative phenomena which extend over a large number of interacting sites. Even within the dodecamer (thought to represent the minimum functional unit), tertiary structural changes induced by the binding of oxygen or CO may affect the four hemes in a tetramer at first and then extend to the dodecamer. Two interesting questions arise from the data summarized above:

† This work was partially supported by the MURST of Italy (40% "Liverprotein" to M.B.) and by the U.S. Public Health Service Grant GM14276 (to Q.H.G.).

* Address correspondence to Andrea Bellelli, Dipartimento Di Scienze Biochimiche, Universita La Sapienza, P. 24 A. Moro 5, 00185 Roma, Italy.

‡ Cornell University.

[1] Abbreviations: Chl, chlorocruorin; Hb, hemoglobin; Mb, myoglobin.

0006-2960/93/0432-7635$04.00/0

how many functionally significant states are required to account for the properties of Chl, and how rapidly do these states interconvert?

The current information about ligand binding to Chl is insufficient to answer these questions, and the kinetic description of ligand-binding and ligand-linked conformational changes in even less complete, being limited to preliminary information reported by Brunori et al. (1965) and to a very recent contribution by Gibson et al. (1992).

In view of the increased knowledge on the structure of these giant respiratory proteins, and because of the improvement in the acquisition and analysis of kinetic results, we undertook a thorough characterization of oxygen and CO binding to Chl from *S. spallanzanii*, with the aim of describing the allosteric properties of this complex system which is able to transfer information over a large cooperative unit. The presence of nested allosteric structures might cause slow and complex transitions, and indeed some hemocyanins are characterized by slow allosteric transitions and tertiary as well quaternary regulatory phenomena [e.g., proton binding; see Zolla et al. (1986)]. In general terms one might expect some correlation between the rate of the allosteric transition, the average distance between the heme groups, and the dimensions of the cooperative unit, and it has already been suggested that the change of reactivity in the homodimeric hemoglobin from *Scapharca inaequivalvis* is much faster than in tetrameric hemoglobins. Our results confirm that some allosteric transition in Chl is slow and populates stable or long-lived intermediates.

MATERIALS AND METHODS

The hemolymph of *S. spallanzanii* worms, collected in the Naples bay, Italy, was extracted from the vessels at the base of the crown in 0.02 M Tris buffer pH 7.5 containing 0.2 M NaCl and 0.001 M EDTA. Chl was purified by sedimentation in a preparative ultracentrifuge (Antonini et al., 1962a) and used within 3 weeks or stored at −80 °C.

The purity of our protein preparations was checked by analytical ultracentrifuge using a Beckman Spinco Model E ultracentrifuge and by analytical fast protein liquid chromatography (FPLC) using the prepacked Pharmacia MonoQ columns.

The heme iron of Chl may undergo oxidation to yield ferric Chl, a scarcely stable derivative which is readily transformed into a stable hemichrome and dissociates into oligomeric aggregates (Ascoli et al., 1981). The presence of met Chl was checked spectrophotometrically, and partially oxidized samples were discarded; the met Chl fraction of the samples used did not exceed 5% and was observed in some experiments by the SVD procedure (see below).

The protein undergoes irreversible dissociation at acid or very alkaline pH; therefore, the present characterization was carried out only over the limited pH range 7.0 to 8.5; where not otherwise specified, the experimental conditions are as follows: 0.05 M Tris–Bistris buffer pH 7.4 containing 0.2 M NaCl, 5 mM $CaCl_2$, and 5 mM $MgCl_2$, 20 °C.

The concentration of the protein was determined spectrophotometrically, using the extinction coefficient of 135 L/mM·cm at 438 nm (Antonini et al., 1962b) for the carbonmonoxy derivative or 2.2 mL/mg·cm at 280 nm.

Oxygen binding isotherms have been recorded using the methods described by Rossi Fanelli & Antonini (1958), Imai (1973), and Gill (1981); these gave superimposable results.

Stopped-flow experiments were carried out either with a Gibson Durrum stopped-flow apparatus connected to a CompaQ 286 computer for data collection (Olis) or with a Tracor Northern rapid scanning photodiode array spectrophotometer adapted to a modified Gibson Durrum apparatus; in the latter case spectra of 1024 points covering a 300-nm wavelength range were collected every 10 ms and transferred to a MicroVax 3500 computer for analysis. The singular value decomposition algorithm was applied to deconvolute spectra, and the columns of V matrix were fitted to the desired kinetic model (Henry & Hofrichter, 1992).

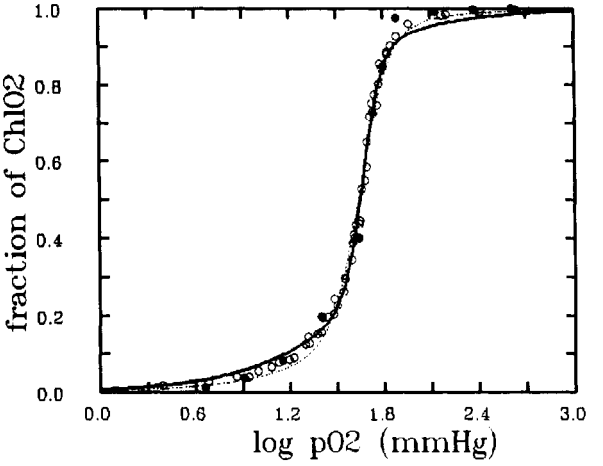

FIGURE 1: Oxygen binding curves of Chl recorded at pH 7.4 in 50 mM Tris/BisTris buffer containing 0.2 M NaCl, 5 mM $MgCl_2$, and 5 mM $CaCl_2$ using the tonometric (○) or the thin-layer dilution methods (●); t = 20 °C. The best fit according to the two-state model (Monod et al., 1965) with a cooperative unit of six sites (dotted line) or 12 sites (continuous line) is also shown.

Flash photolysis experiments (70-μs pulse) were carried out with an apparatus similar to that described by Brunori and Giacometti (1981). Photolysis of ChlCO and $ChlO_2$ was also obtained by means of a YAG laser (Quantel model 571, Santa Clara, CA), which delivers 35-ps or 9-ns quasi-Gaussian light pulses at 532 nm. The time course of ligand rebinding after photolysis was followed in the ps to ms range as previously described (Bellelli et al., 1990).

The apparent quantum yield was determined from the laser photolysis experiments exploiting the linear correlation between the logarithm of the liganded Chl and the light used for photolysis, using sperm whale myoglobin CO as a quantum yield = 1 standard and correcting the result for the ratio of the extinction coefficients of ChlCO (or $ChlO_2$) and MbCO (Saffran & Gibson, 1977).

The kinetics of oxygen relase were followed by three different techniques: (i) mixing oxygenated Chl with sodium dithionite; (ii) mixing a solution of dithionite containing Chl with oxygen equilibrated solutions (oxygen pulse technique; Gibson, 1974); and (iii) mixing oxygenated Chl with carbon monoxide (replacement reaction; Antonini and Brunori, 1971).

The kinetics of carbon monoxide dissociation were studied by mixing ChlCO with excess microperoxidase (Sigma), as described by Sharma et al. (1976).

The experimental data were collected by or transferred to an IBM PC/AT and fitted to the desired model using the Marquardt algorithm (Marquardt, 1963).

RESULTS

Oxygen Binding. Oxygen binding to Chl is cooperative; the binding isotherms, shown in Figure 1, are easily described in the framework of the two-state allosteric model (Monod et al., 1965), assuming that cooperative effects involve either six or 12 ligand binding sites. The oxygen affinity of Chl

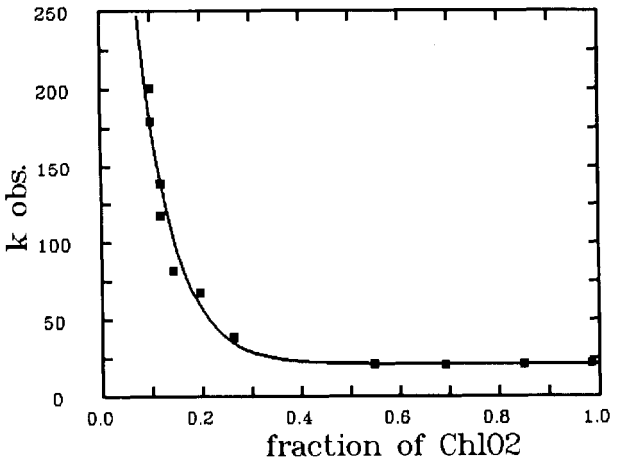

FIGURE 2: Oxygen pulse experiment. Chl in a buffered solution of $Na_2S_2O_4$ was mixed with oxygen-containing buffer (from 35 to 760 mmHg), and the reaction was followed at 455 nm. The observed rate constant is plotted as a function of the fractional saturation achieved before O_2 dissociation begins (Y). Conditions: 50 mM Tris/BisTris buffer containing 0.2 M NaCl, 5 mM $MgCl_2$, and 5 mM $CaCl_2$, pH 7.4, t = 20 °C.

displays a marked pH dependence, the Bohr coefficient (Δ log $p^1/_2/\Delta$pH) being –0.45 between pH 7.5 and 8.2 [in agreement with Antonini et al. (1962a)]; as in mammalian hemoglobins the average value of the Hill coefficient is only marginally affected by pH. Unfortunately, irreversible dissociation into subunits occurs at more extreme pH values, hindering a better definition of the Bohr effect (Antonini et al., 1962a).

Cooperativity in the oxygen dissociation reaction could be demonstrated in an "oxygen pulse" experiment (Gibson, 1974). In this experiment a solution of unliganded Chl containing excess dithionite is mixed in a stopped-flow apparatus with oxygen-containing buffer; in view of the two parallel and competing reactions (oxygen binding to Chl and oxygen reduction by dithionite), the extent of oxygen saturation achieved during the pulse may be modulated by systematically varying the concentrations of oxygen and dithionite. The presence of a large excess of dithionite ensures that oxygen dissociation rates from partially or fully saturated Chl can be followed at the end of the pulse.

On varying the oxygen saturation at the end of the oxygen pulse between 10% and 100% (as estimated from the optical density change) it was observed that the first-order rate constant for oxygen dissociation varied monotonically from >200 s^{-1} to 15 s^{-1}, as shown in Figure 2. Given the shape of the O_2 binding isotherm (with extended n = 1 asymptotes), the lowest oxygen saturation levels achieved do not promote the full allosteric transition; hence, the protein remains in the T state and rapid oxygen dissociation occurs (k > 200 s^{-1}). It is important to point out that complete recovery of the expected optical density change was obtained in oxygen pulse experiments carried out at high oxygen concentration, a demonstration that oxygen binding (though slow as compared with mammalian hemoglobins, see below) is still relatively fast.

When Chl is fully saturated with the ligand (1 atm O_2 before mixing), oxygen dissociation in the pulse experiment is slow (k = 15 s^{-1}). Likewise, on mixing 95% saturated $ChlO_2$ (in equilibrium with air) with dithionite, the first-order rate constant of oxygen dissociation is slow (k = 10 s^{-1}). Therefore at the high O_2 concentrations necessary to approach full saturation in an oxygen pulse experiment, a high affinity state is fully populated within 10–20 ms, implying that the T to R transition occurs on a faster time scale.

Table I: Equilibrium and Kinetic Constants Describing the Reaction of Chl with Oxygen[a]

KR	KT	L_0	kR	kT
7	140	2×10^8	15	>200
	k' fast	$k'R$	$k'X$	$k'T$
stopped flow				0.3×10^6
flash		1.5×10^6		
laser	9.6×10^6	1.5×10^6		
calcd		2.1×10^6		$>1.4 \times 10^6$

[a] Fitting was run under the assumption of a two state model with a cooperative unit of 12 oxygen binding sites (from Figure 1). Experimental conditions: Tris/BisTris buffer, pH 7.4, 20 °C. The equilibrium constants (K) are expressed as dissociation constants in μmol O_2/L; the combination rate constants (k') are in $M^{-1}\cdot s^{-1}$; the dissociation rate constants (k) are in s^{-1}.

In experiments carried out mixing $ChlO_2$ with dithionite, a slower optical transition, opposite in sign to the main process, was sometimes observed at 605 nm and confirmed by the presence of a second component in the SVD analysis of the time-resolved spectra (500–650 nm). This second kinetic component, not present in oxygen pulse experiments, may be due to the slow reduction of small amounts of ferric Chl (as judged from the position of the peaks observed in the second column of the U matrix).

The most important piece of information which emerges from comparison of the data in Figure 2 with the results illustrated above, is that the switchover point calculated from equilibrium experiments (i.e., Y = 0.54, with an almost symmetrical binding curve) corresponds to a much higher degree of ligation than that estimated from the kinetic data (Y = 0.2); not only the populations of the R and T states are far from equilibrium during the reactions studied, in contrast to human Hb (Hopfield et al., 1971), but in order to account for the earlier switchover, some intermediate species must be populated in the kinetic experiments. An interpretation, based also on the CO combination kinetic data reported below, is presented in the Discussion.

From the parameters of the fit to the oxygen binding isotherm and the oxygen dissociation rate constants for the T and R states, we estimated the rate constants for oxygen combination (see Table I); the calculated values are sufficiently low to encourage a direct determination, either by partial photolysis for the R state or by stopped-flow for the T state.

Oxygen binding to the R state after partial photolysis (5–25%, using the 70-μs flash), obtained in the presence or in the absence of CO, gives a single exponential and yields a second-order rate constant (1.5×10^6 $M^{-1}\cdot s^{-1}$) very close to the calculated value (Table I).

In contrast, the time course of oxygen binding to unliganded Chl, recorded in a stopped-flow apparatus, is complex, as shown in Figure 3. At very low oxygen concentration the time course is described for 85% of the optical transition by a single exponential (11 s^{-1} at 35 μM O_2), while at intermediate to high O_2 concentrations the time course is more clearly biphasic and depends on ligand concentration with an order lower than 2. The relative amplitude of the two phases does not show a simple dependence on oxygen concentration.

The overall half time of the reaction estimated from these data is approximately 1 order of magnitude greater than the calculated one; i.e., the highest estimate of k', obtained from the time courses recorded at the two lowest values of pO_2 (35 and 68 μM) is 0.3×10^6 $M^{-1}\cdot s^{-1}$, the value tentatively assigned

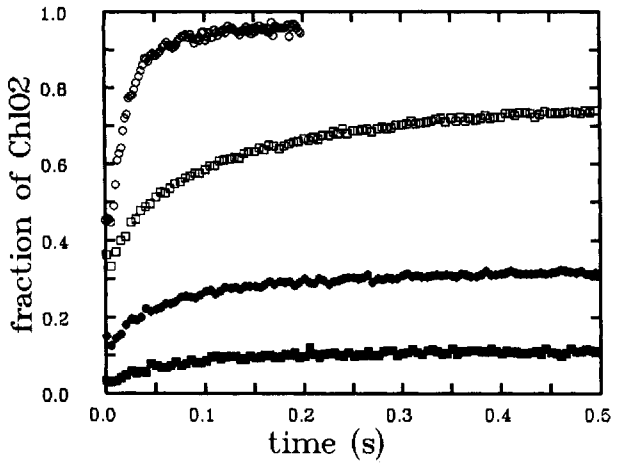

FIGURE 3: Oxygen binding to deoxygenated Chl recorded by stopped flow at 455 nm. Chl concentration was 4 μM (per heme, after mixing); other conditions as in Figure 2, except for the oxygen concentrations, as follows: (■) 35 μM; (●) 70 μM; (□) 135 μM, and (○) 670 μM.

Table II: Kinetic Constants Describing the Reaction of Chl with CO[a]

	l overall	*l'* fast	*l'R*	*l'X*	*l'T*
stopped flow	0.0035				7×10^4
flash			4×10^5	1.4×10^5	7×10^4
laser		8.4×10^6	7.4×10^5		8.4×10^4

[a] Experimental conditions: Tris/BisTris buffer pH 7.5, 20 °C. The combination rate constants (*l'*) are in $M^{-1}s^{-1}$; the dissociation rate constants (*l*) are in s^{-1}.

to *k'T* in Table I; we are not able at present to explain the difference with the calculated value.

The analysis of O_2 combination is made more difficult by the incomplete recovery of the expected optical transition, due to complexities inherent in the experimental procedures. Although the samples were not fully deoxygenated to begin with, at high oxygen concentrations (0.65–0.13 mM) a very fast ligand binding event, attributed to the rapid equilibration of T state Chl and lost in the dead time of the stopped-flow apparatus, precedes a biphasic reaction leading to complete saturation (with an apparent rate constant for the faster process of 60 s^{-1} at 0.65 mM O_2). As discussed below, T-state oxygen binding was not observed in experiments carried out using laser photolysis.

Carbon Monoxide. The affinity of Chl for carbon monoxide is reported to be high (Fox, 1932); therefore, we did not attempt to record an equilibrium binding curve directly because the dilution required would be extreme, while the optical transition is smaller than in hemoglobins. We estimated, instead, the partition constant between oxygen and carbon monoxide (Antonini & Brunori, 1971) and observed that it is characterized by a heterogeneous behavior (possibly due to differences in cooperativity in the binding of these two ligands; see below); thus, only a lower limit of $K_{O_2}/K_{CO} = 0.01$ was obtained for the partition constant (expressed as the ratio of the dissociation constants). This value is consistent with the kinetic analysis.

Carbon monoxide combination with unliganded Chl has been followed by stopped-flow and by 70-μs flash photolysis. The time course of CO combination is either slightly autocatalytic or single exponential by both techniques (provided that photolysis yields fully photodissociated Chl, as judged by optical spectroscopy); the rate constant is second order.[2]

The experiments in which photolysis is obtained with the 70-μs flash yield no observable geminate kinetic components,

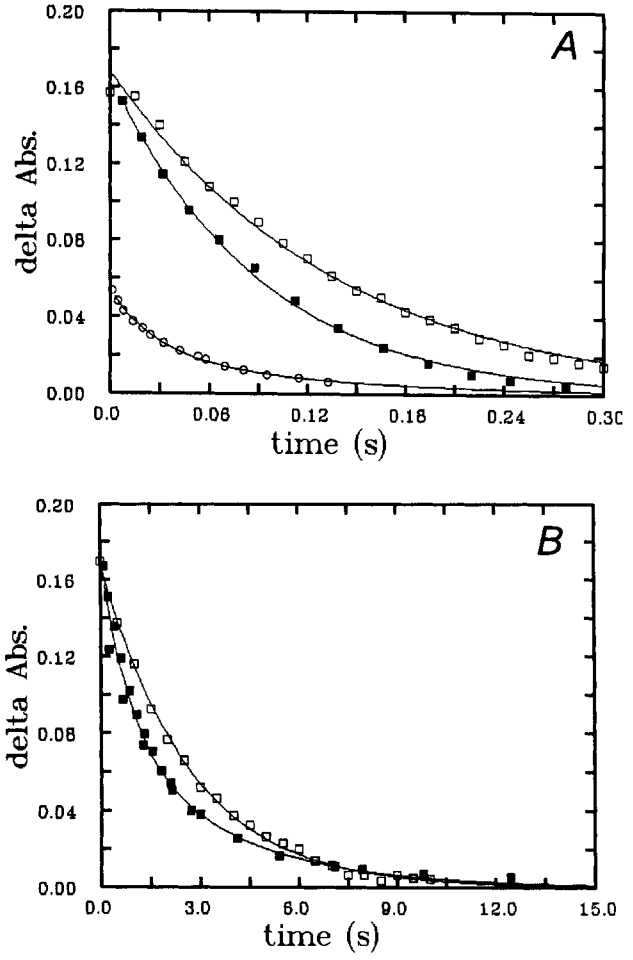

FIGURE 4: Time course of carbon monoxide binding to Chl. Experimental conditions: 0.05 M Tris/BisTris buffer pH, 7.4, containing 0.2 M NaCl, 5 mM $CaCl_2$, and 5 mM $MgCl_2$; protein concentration 1 μM (both panels); CO concentration 100 μM (panel A) or 6.2 μM (panel B); light path = 2 cm; λ = 455 nm. Flash photolysis experiments are indicated as follows: ■ = full photolysis; ○ = 30% photolysis; □ = stopped flow experiments. Continuous lines are the best fits to a single exponential (■ and □ in 4A, □ in 4B) or to two exponentials (○ in 4A and ■ in 4B).

contrary to those in which photolysis is obtained with a 9-ns or a 35-ps laser pulse (see the following section).

The time course of CO rebinding to partially photolyzed (down to 5%) Chl is biphasic; the rate observed in these experiments (Figure 4), which populate partially liganded and presumably R state intermediates, is 2–3-fold higher than that seen in full photolysis and significantly lower than that of R state Hb.

In summary, the rate constant for CO combination, determined by mixing deoxygenated Chl with carbon monoxide, is smaller (by at least a factor of 2) than that measured after full photolysis of the CO derivative (with a 70 μs flash), which in turn is two to three times slower than the faster rate measured after partial photolysis with the same flash; thus, three CO combination rates may be clearly distinguished. The data in Figure 5 shows the second-order rate constant measured with the three techniques as a function of CO concentration; the averaged values are reported in Table II.

[2] We have never seen any evidence for a quickly reacting species analogous to that observed by full photolysis with hemoglobin and attributed to $\alpha\beta$ dimers (Gibson & Antonini, 1967); it may be recalled that Chl shows no sign of reversible dissociation into subunits in ultracentrifuge experiments at neutral pH (Antonini et al., 1962b).

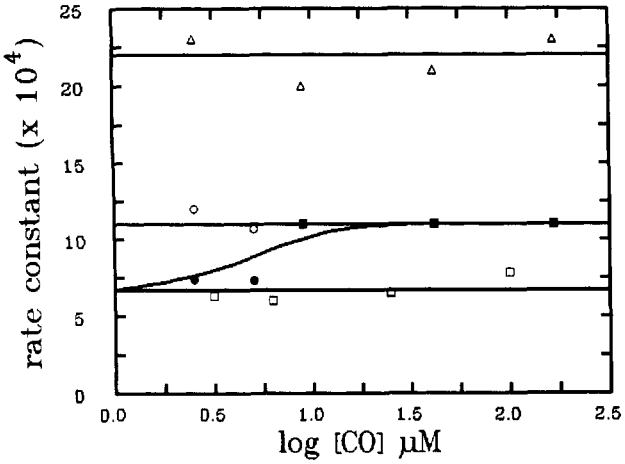

FIGURE 5: Correlation between the second-order rate constant for CO combination and the concentration of the gas. Experimental conditions as in Figure 4. Rate constants (in $M^{-1}\cdot s^{-1}$) were obtained by partial photolysis (△), full photolysis (■, ○, and ●) and stopped flow (□). The symbols ○ and ● refer to the two rate constants necessary to describe the heterogeneous time course recorded by flash photolysis at low [CO] (see Figure 4B).

Three second-order rate constants imply three reactivity states; moreover, the finding of a homogeneous time course in the stopped-flow experiments suggests that even with the long light pulse (70 μs) yielding complete photodissociation, deoxy Chl had no time to relax fully to a stable deoxy conformation (unliganded T state) before ligand recombination from the bulk (Figure 4A). The situation is clarified by additional flash photolysis experiments carried out by progressively diluting the ligand (and the protein, if necessary, to maintain a pseudo first-order kinetics) down to 2.5 μM (and 0.3 μM Chl). When the concentration of CO was lower than 10 μM, a biphasic ligand rebinding to fully photolyzed Chl was observed, as shown in Figure 4B. The two kinetic components of the time course under these conditions have rate constants identical to the reactions observed in stopped-flow and full photolysis experiments at high [CO], respectively; thus, the second-order rate constant for CO binding to Chl after full photolysis depends on ligand concentration, as shown in Figure 5. This is consistent with the hypothesis of a slow ($t_{1/2}$ = ~1 s) decay of the fully photolyzed deoxy Chl to the equilibrium deoxy Chl.

Carbon monoxide dissociation from ChlCO was followed by mixing with an excess of microperoxidase [see Sharma et al. (1976)]; the overall first-order rate constant (0.0035 s^{-1}) is lower than that of R-state Hb (0.009 s^{-1}; Sharma et al., 1976).

Geminate Ligand Rebinding and Difference Spectra of Photolyzed Chlorocruorin. The reaction of *Spirographis* Chl with oxygen and carbon monoxide was also followed over the ps to ms time regime using laser flashes of 35-ps and 9-ns duration: the flashes are shorter than the time taken by some ligand molecules to diffuse through the protein into the solvent. After the pulse these trapped molecules may rebind to the heme iron in one (or more) rapid first-order rebinding reaction, a phenomenon called "geminate recombination", and extensively studied in hemoglobins and myoglobins (Hofrichter et al., 1983; Gibson, 1990). Geminate rebinding is not seen with the 70-μs flash whose rate of photochemical work is not sufficiently high to give a significant population of the short-lived geminate states, so that only ligand molecules which have diffused into the solvent during the flash can be seen to rebind.

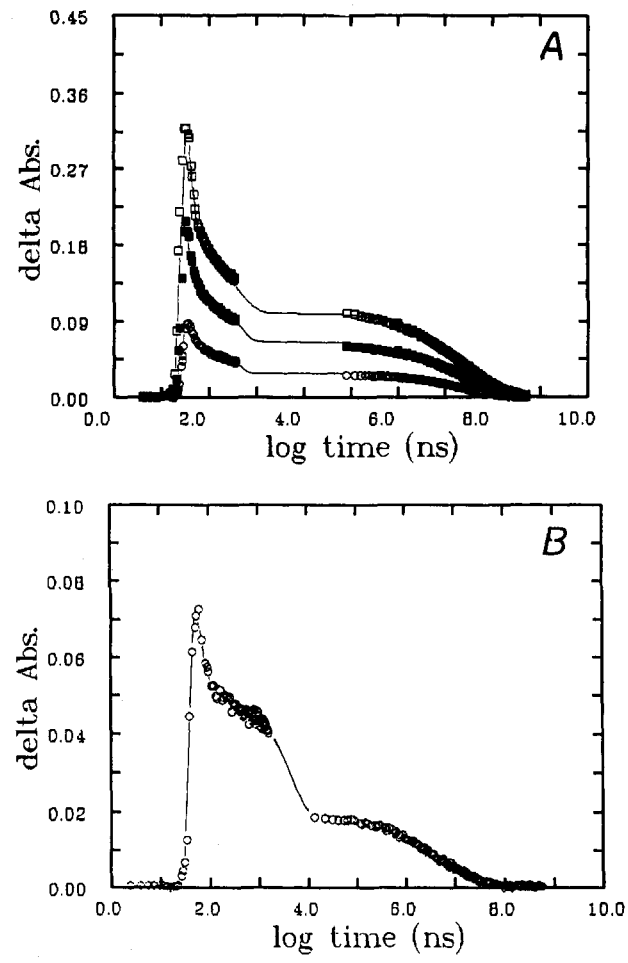

FIGURE 6: Time course of CO (panel A) and oxygen (panel B) rebinding to Chl after photolysis obtained with the 35-ps and 9-ns laser pulse. The logarithmic time scale allows the geminate and bimolecular phases to be represented in the same plot. Panel A: □, ChlCO, full intensity of the photolyzing light and 70% photolysis; ■, 1/8 of the maximal photolyzing light (45% photolysis); ○, 1/32 of the maximal photolyzing light (20% photolysis). Panel B: ○, $ChlO_2$, full intensity of the photolyzing light and 15% photolysis. Experimental conditions: 85 μM Chl, 0.1 atm CO or O_2, 0.1 M BisTris buffer pH 7.0, t = 20 °C. Total expected absorbance changes at the observed wavelength (455 nm): 0.45 for ChlCO (full scale of the ordinate), 0.48 for $ChlO_2$.

An extended time course, encompassing the geminate and bimolecular rebinding phases observed after photolysis of ChlCO with a 9-ns laser pulse is depicted in Figure 6A, which also shows that the peak population of unliganded Chl corresponds to 70% of the total concentration of the pigment (the maximum of the absorbance scale of Figure 6A represents the static difference).

After the 9-ns laser pulse, rebinding of CO to Chl displays two well-resolved first order processes (Figure 6A) in the tens of ns time scale, with rate constants of 77 × 10^6 s^{-1} and 2.9 × 10^6 s^{-1}; their relative amplitude is independent of the extent of photolysis and corresponds to 41 and 27% of the recorded absorbance change; the remaining 32% of the CO photolyzed rebinds from the solvent.

The incomplete photolysis is attributed to ligand rebinding on a time scale of tens of ps, i.e., fast enough to compete with photolysis by the 9-ns pulse. This was shown directly in experiments carried out with a 35-ps laser pulse: in this case a significant amount of the photolyzed ligand (35%) rebinds with a rate constant of 3 × 10^9 s^{-1}, and the yield of photolysis at the peak of the laser pulse is now close to 100% (data not shown). Since the relative amplitude of the geminate processes

depends on the length of the laser pulse, while their rates do not, this datum cannot be immediately compared with those reported in Figure 6A; moreover, the observing wavelength for the ps experiment (which is fixed at 436 nm because of the construction of the instrument) is unfavorable for *Spirographis* Chl, due to the spectral properties of the chloro-heme (see also below).

The three first-order processes observed with the 35-ps and 9-ns laser pulses are attributed to rebinding from inside the protein matrix (geminate rebinding) on the basis of the independence on the concentration of CO and of the overall spectroscopic features. The simplest interpretation of three distinct geminate states of each subunit is, however, complicated by the possible existence of intramolecular heterogeneity.

Three second-order phases were seen after the 9-ns laser pulse, with rate constants of 8.4×10^6 $M^{-1}\cdot s^{-1}$, 0.74×10^6 $M^{-1}\cdot s^{-1}$ and 0.084×10^6 $M^{-1}\cdot s^{-1}$; the two slower processes correspond closely to those observed by partial photolysis (with the 70-μs flash) and stopped-flow respectively. The relative amplitude of these phases is almost independent of the extent of photolysis: they account for 6, 13.5, and 12.5% of the total absorbance change expected (see Figure 6A).

It is important to note two differences between laser photolysis and the slower kinetic techniques (stopped-flow and the 70-μs flash photolysis): first, in the laser experiments there is an additional second-order process faster than that observed with the 70-μs pulse (a very fast bimolecular process is also present in the case of oxygen; see below), and second, a finite amount of equilibrium T-state Chl is detected in the laser experiments, in spite of the lower photolysis level and the geminate rebinding. By contrast, the intermediate phase observed in 70-μs flash photolysis experiments, which corresponds neither to T nor to R, is absent. These differences will be discussed below.

Chl from *Spirographis* is poorly light sensitive; in fact, the apparent quantum yield for CO is 40% at 35 ps and only 14% at the peak of the 9-ns laser pulse; whether this is due to an intrinsically low yield or to an extremely fast transient competing with the photolysis [see, for example, Petrich et al. (1989)] is unclear.

Analysis of the oxygen data is more difficult, due to the even lower apparent quantum yield; for example, after the 9-ns laser pulse the apparent photochemical yield was 15%. Two geminate phases were observed, with rate constants similar to those reported for CO, followed by two bimolecular phases with the rate constants of 9.6×10^6 $M^{-1}\cdot s^{-1}$ and 1.5×10^6 $M^{-1}\cdot s^{-1}$ (see Figure 6B). As in the case of CO, the faster component is faster than that measured with the 70-μs flash and is also faster than that calculated for the R state; T-state reactivity is not detected. The 35-ps laser pulse yields a low fraction of photolysis (=50%) and shows a fast geminate phase (with a rate constant of 12×10^9 s^{-1}), accounting for over 75% of the observed absorbance change.

The kinetic difference spectrum of ChlCO versus deoxy Chl at 9 and 400 ns corresponds to the static difference spectrum in the region 470–435 nm; however, the appearance of a novel difference peak at 420 nm implies that an additional transient species is populated by the laser pulse and decays in the μs time range (ChlCO is shown in Figure 7; $ChlO_2$ is not shown). No analogous peak has been observed in hemoglobins or in the Chl from *E. vancouverii* (Gibson et al., 1992). Population of this novel transient continues into the μs time regime and complicates the interpretation of the geminate processes, some of which may not correspond to the rebinding properties of equilibrium states of Chl. It is uncertain whether the new spectroscopic component and the fastest bimolecular process can be traced to the same intermediate, since their time scales do not coincide exactly.

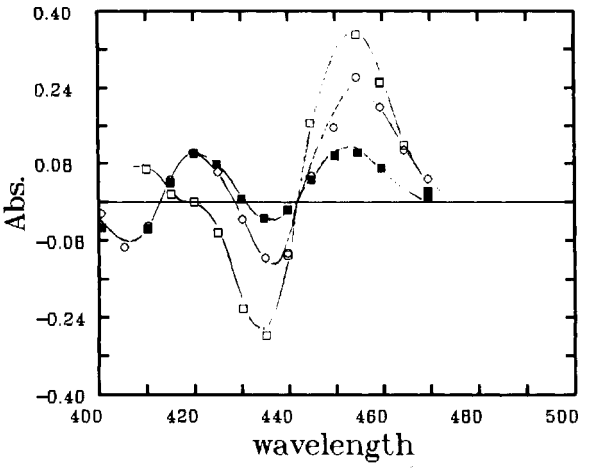

FIGURE 7: Difference spectra of Chl after photolysis (taking ChlCO as the reference): ○ = 70% photolyzed Chl (peak of the 9-ns laser pulse); ■ = Chl after the geminate rebinding phases (spectrum collected 400 ns after the laser pulse; ChlCO 70%, Chl 30%); □ = Chl at the beginning of the bimolecular rebinding phases (20 ms; the amplitude has been multiplied by 10). The spectrum collected at 20 ms is closely superimposable in shape to the static difference spectrum [Chl − ChlCO]. Experimental conditions: light path 1 mm, 85 μM Chl (per heme), 1 atm CO, 0.1 M BisTris buffer pH 7.0, t = 20 °C.

DISCUSSION

The equilibrium and kinetic ligand binding parameters reported above allow us to propose a detailed description of the reactions of Chl from *S. spallanzanii* and clearly indicate that, under some experimental conditions, the allosteric transition(s) lags behind the binding and dissociation of the ligands (O_2 and CO). Moreover, at least one long-lived and functionally distinct intermediate is populated. The rates of the allosteric transitions must, therefore, be taken into account explicitly, leading to a kinetic scheme with a minimum of three significantly (even if transiently) populated states called T, X, and R.

The Kinetic Scheme. The minimal kinetic scheme may be written as:

Scheme I

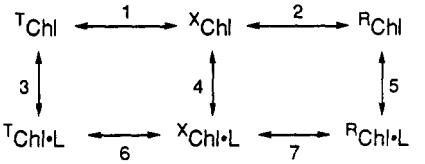

As discussed below, X needs not to be a stable allosteric state and may correspond to a long-lived kinetic intermediate. Reactions 3–5, representing ligand binding to and release from the T, X, and R states of Chl, are relatively fast and correspond to the elementary chemical processes. The combination rate constants are given in Tables I and II.

The transition from the T to the R state (and vice versa) both in unliganded and (partially) liganded Chl is slow and takes place *via* the state X characterized primarily by a CO reactivity in between that of the T and R states. Photolysis of CO from the R state yields ^{R}Chl which relaxes to ^{X}Chl (by reaction 2, which is complete in 70 μs); this derivative may in turn decay to unliganded ^{T}Chl (by reaction 1, which takes seconds) or react with the ligand and return to the liganded R state (reactions 4 and 7), depending on the relative rates of the two competing processes.

The rate of the bimolecular CO binding to Chl measured by photolysis (using the 70-μs flash) is twice as fast as that measured by stopped flow, if [CO] is greater than or equal to 10 μM. Assuming that the stopped-flow technique measures the combination rate of ^{T}Chl and partial photolysis that of ^{R}Chl, the rate of CO rebinding to fully photolyzed Chl has been assigned to X. Upon extreme dilution of the reactants, the reaction observed after photolysis becomes biphasic, the reactivity of the slower component corresponding now to that of the T state (Figure 4 and Table II). These data suggest approximate time scales for the structural changes: ^{R}Chl $\rightarrow$ ^{X}Chl (which occurs during the 70-μs flash) and ^{X}Chl to ^{T}Chl (with a rate constant of 0.7–1 s^{-1} from the experiments of Figures 4 and 5).

The transitions in the opposite direction (along the pathway T $\rightarrow$ X $\rightarrow$ R) cannot be studied directly in unliganded Chl but are proposed to be first-order and relatively slow in the liganded derivatives. At least one of them may be rate limiting in the course of oxygen combination. Thus, in the rapid mixing experiment with pure O_2 (Figure 3), $Y = 0.5$ is achieved in the dead time of the apparatus and corresponds to the expected partial saturation of ^{T}Chl, while the observed process ($k = 60$ s^{-1}) may reflect the $X_i \rightarrow R_i$ transition which limits the rate of further binding of O_2.

Finally, two structural transitions, involving the intermediate X state, may explain the low apparent switchover point (2.4/12) recorded in the oxygen pulse experiment (Figure 2). In this case all three states may be populated at different levels of saturation with oxygen; however, if the rate of oxygen dissociation from the X state were close to that of the R state, only two rates would be seen and the apparent switchover point would correspond to the T $\rightarrow$ X transition, being thereby (grossly) different from that computed from the oxygen binding isotherm (6.5/12).

Scheme I should apply to *Spirographis* Chl independently of the ligand; however, combination with CO is so slow that under most experimental conditions the T $\rightarrow$ X $\rightarrow$ R transitions are not rate limiting, so the autocatalytic time course observed during stopped flow CO combination is not inconsistent with the biphasic course of oxygen combinatinon (Figure 3).

Our present results are far from sufficient for a complete quantitative description of all the allosteric transitions in Chl; in fact, the number of rate constants in a realistically extended form of Scheme I is huge, given the dodecamer as the functional unit. Moreover, although a three-state scheme provides a satisfactory description of the experimental data, the third state X is described only as a long-lived intermediate, possibly poorly populated at equilibrium (see the discussion of the laser photolysis experiments, below). Thus, although our kinetic data may appear to demand a three-state model, as first proposed by Minton & Imai (1974), fitting the equilibrium experiments with a more complex model seemed unnecessary, given that they are already satisfactorily described by the simple MWC scheme.

A third, transient, state of Chl explains some apparent inconsistences in measurements by different techniques. Because of the long half life of unliganded X state (see above), T state Chl is not populated in 70-μs flash photolysis experiments, even after complete removal of CO and this, within error, implies that in the CO derivative at equilibrium, ^{T}ChlCO, accounts for less than 10% of the total pigment. In contrast, in laser photolysis experiments in which (due to the incomplete photolysis and the geminate rebinding phases) CO rebinds from the solvent to 70% saturated Chl, a phase with the rate constant characteristic of T state Chl is clearly detectable. This difference between the two techniques may be explained assuming that a small but significant (say 5–10%) fraction of ChlCO is in the T state at equilibrium (^{T}ChlCO); the relative weight of the kinetic phase due to this fraction would be negligible in the 70-μs flash photolysis experiments (where all the ligand is removed) but would be a significant fraction of the bimolecular components observed after the 9-ns laser photolysis, since the T state has a lower geminate yield and a higher apparent photosensitivity [data not shown; see also the equivalent data collected on hemoglobin, for example by Saffran and Gibson (1977), Sawicki and Gibson (1979), and Hofrichter et al. (1983)].

T-state reactivity is not observed in laser photolysis experiments carried out on $ChlO_2$; this may be due to the smaller difference in the combination rate of this ligand to the two allosteric states. Moreover, since both allosteric states are expected to have low apparent quantum yields for oxygen, little relative enrichment of T state Chl would be induced by the photochemical event. Finally, oxygen appears to be more cooperative than CO, given that for CO the ratio of the combination rate constants, $l'R/l'T$, expressing kinetic cooperativity, is only 5.7, whereas in the case of oxygen the ratio of the off rate constants, $kT/kR > 13$ and $c = 0.05$ (neglecting the contribution of the on rates; Tables I and II); thus the equilibrium fraction of $^{T}ChlO_2$ is likely to be smaller than that of ^{T}ChlCO.

Two other, more puzzling discrepancies between the 9-ns laser and 70-μs flash photolysis experiments are that (i) the laser pulse induces a distinct and reversible spectroscopic component (characterized by a positive peak centered at 420 nm) and (ii) the rebinding of the ligand (oxygen or CO) from the solvent is characterized by a very fast bimolecular component (9.6 and 8.4×10^6 $M^{-1} \cdot s^{-1}$, respectively, for oxygen and CO), not observed with the 70-μs flash (it is difficult to attribute this rate to an intermediate populated at equilibrium, given the data reported in Table I). Whether these two observations relate to the same molecular phenomenon is uncertain; however, the existence of a photoexcited intermediate, possibly characterized by high ligand reactivity, may account for this observation.

On the nature of this photoexcited intermediate a tentative interpretation is possible along the lines proposed for free heme (Huang et al. (1989)) and for miniMb (Di Iorio et al., 1992). In these cases the laser pulse seems to induce photolysis of the iron–proximal histidine bond, leading to a tetracoordinated metal complex characterized by a peak in the difference spectrum, at wavelength lower than that of the CO–heme complex. Thus, if laser photolysis of the proximal histidine–iron bond occurs also in Chl, this may explain the spectra reported in Figure 7; moreover, the four-coordinate iron is known to exhibit a very high rate of ligand rebinding (Giacometti et al., 1977).

Structural Considerations. The hierarchical organization proposed for the assembly of giant oxygen carriers (Qabar et al., 1992) finds a parallel in the concept of nesting of allosteric states with the definition of a "local T" and "local R" substructures nested into "global T" or "global R" superstructures [see Robert et al. (1987)]. Within this framework the X state may be envisaged as a dodecamer containing a mixture of T- and R-state tetramers and thereby may account for the main results which emerged from this investigation, i.e., a possible correlation between the average dimension of the allosteric functional unit and the rate constant of the quaternary allosteric transition.

Kinetic data for tetrameric hemoglobins, analyzed within a two-state allosteric model, yield a relaxation rate constant for the R ↔ T transition which depends on the number of ligands bound to the tetramer and range from 100 000 s^{-1} ($R_0 \rightarrow T_0$) in the deoxygenated protein to 3000 s^{-1} ($R_3 \leftrightarrow T_3$) in the triply-liganded hemoglobin (Sawicki & Gibson, 1976; Ferrone & Hopfield, 1976; Hofrichter et al., 1983). These relaxations are usually much faster than the bimolecular recombination of the ligand from the solvent.

Crystallographic studies have shown that the T → R conformational change involves a reorganization of the $\alpha_1\beta_2$–$\alpha_2\beta_1$ interfaces, while the other contact surfaces are essentially rigid (Perutz, 1970; Baldwin & Chothia, 1979). Thus, the largest structural change (sliding of the $\alpha_1\beta_2$ surface and relative rotation of the two $\alpha_1\beta_1/\alpha_2\beta_2$ dimers) corresponds to the concerted motion of the two dimers, with heme–heme "information transfer" over an average distance of at least 25 Å. The optical change in the deoxy state associated with the T–R transition (Sawicki & Gibson, 1976; Hofrichter et al., 1983) has been convincingly correlated to the structural change seen by crystallography and is synchronous with the resonance Raman shift of the peak assigned to the tryptophanyl residue at position β37 [located at the $\alpha_1\beta_2$ interface, see Su et al. (1989) and Kaminaka et al. (1990)].

While the relaxation time of the $R_0 \rightarrow T_0$ allosteric transition for several tetrameric hemoglobins is in the time range of the ms (e.g., Hofrichter et al., 1991), the homodimeric hemoglobin from *Scapharca inaequivalvis*, in which close distance between the heme groups has been demonstrated by X-ray crystallography (Royer et al., 1990), undergoes a reactivity change in a time range of ns (Chiancone et al., 1993); thus, the shorter heme–heme contact distance is associated to a smaller and faster structural transition coupled to the control of the ligand binding.

Giant respiratory proteins, such as Chl, afford a good or unique opportunity to extend the correlation between the rate of the allosteric transition and the dimension of the protein super domain involved in the functional unit; such a correlation was proposed several years ago on the basis of rapid kinetic experiments on hemocyanins from molluscs and arthropods (Kuiper et al., 1977; Van Driel et al., 1978). Analysis of oxygen-binding data of Chl by Colosimo et al. (1974) has shown that the ligand-linked conformational change which mediates cooperativity, though not extending over the whole assembly (3 MDa and 96–156 hemes), occurs in a cooperative mode within a functional unit of 10 sites. Imai's (1985) analysis led to an estimate of six sites in the functional unit of Chl from *Potamilla*, which, however, may be difficult to extend to the case of *Spirographis* Chl because under some experimental conditions the maximum Hill coefficient is as high as $n = 6$ (Antonini et al., 1962a).

The structure proposed for Chl from *E. vancouverii* supports the dodecamer as the functional unit; the myoglobin-like monomers are, however, assembled in disulfide-bonded tetramers, and the assembly of three tetramers builds up the dodecamer (Qabar et al., 1991). Thus, even though the heme–heme distance in the tetramer is possibly similar to that in human hemoglobin, the transfer of information between the hemes in a dodecamer is likely to be uneven, each subunit interacting more strongly with the other subunits of the same tetramer.

It is interesting to suggest that, as the rate of the R_0 to X_0 transition in Chl is similar to that of the R_0 to T_0 transition in hemoglobin, this process may be attributed to the structural relaxation of the tetrameric substructure within Chl; by contrast, the long-lived intermediate observed in the kinetics analyzed above may correspond to some transient combination of liganded and unliganded tetramers in the dodecamer (or in the whole macromolecule) with a considerable kinetic barrier for the reorganization to the equilibrium quaternary structure.

In conclusion, comparison of the kinetic parameters of *Spirographis* Chl with those of hemoglobins demonstrates a correlation between the average dimension of the allosteric functional unit and the overall rate of the relevant quaternary transition, the relevant time domain being seconds for Chl, ms for human Hb, and ns for dimeric *Scapharca* Hb (which, however, undergoes a more limited structural rearrangement). This result puts on a firmer basis the hypothesis previously formulated from a comparison of hemocyanins from different species (Van Driel et al., 1974; Van Driel et al., 1978), i.e., that giant respiratory proteins may display very slow allosteric transitions. After all, an elephant cannot dance like a kitten.

ACKNOWLEDGMENT

We are grateful to Mr. Pasquale Sansone, Stazione Zoologica, Naples, Italy, who provided the biological samples. Stimulating discussions with Dr. W. A. Eaton (NIDDK, Bethesda, MD), E. Di Iorio (ETH, Zurich, Switzerland), and S. N. Vinogradov (Wayne State University, Detroit, MI) are gratefully acknowledged.

REFERENCES

Antonini, E., & Brunori, M. (1971) *Hemoglobin and myoglobin in their reactions with ligands*, North Holland, Amsterdam.

Antonini, E., Rossi Fanelli, A., & Caputo, A. (1962a) *Arch. Biochem. Biophys. 97*, 336–342.

Antonini, E., Rossi Fanelli, A., & Caputo, A. (1962b) *Arch. Biochem. Biophys. 97*, 343–350.

Ascoli, F., Rossi Fanelli, M. R., Chiancone, E., & Antonini, E. (1981) in *Structure, active site and function of Invertebrate oxygen binding proteins* (Lamy, J., & Lamy, J., Eds.), pp 517–526, Marcel Dekker, New York.

Baldwin, J., & Chothia, C. (1979) *J. Mol. Biol. 129*, 175–220.

Bellelli, A., Blackmore, R. S., & Gibson, Q. H. (1990) *J. Biol. Chem. 265*, 13595–13600.

Brunori, M., & Giacometti, G. M. (1981) *Methods Enzymol. 76*, 582–595.

Brunori, M., Guerritore, D., Antonini, E., Wyman, J., & Rossi, Fanelli, A. (1965) *Pubbl. Staz. Zool. Napoli 34*, 521–527.

Chiancone, E., Elber, R., Royer, W. E., Jr., Regan, R., & Gibson, Q. H. (1993) *J. Biol. Chem. 268*, 5711–5718.

Colosimo, A., Brunori, M., & Wyman, J. (1974) *Biophys. Chem. 2*, 338–344.

Di Iorio, E., Yu, W., Calonder, C., Winterhalter, K. H., De Sanctis, G., Falcioni, G., Ascoli, F., Giardina, B., & Brunori, M. (1993) *Proc. Natl. Acad. Sci. U.S.A. 90*, 2025–2029.

Ferrone, F. A., & Hopfield, J. J. (1976) *Proc. Natl. Acad. Sci. U.S.A. 73*, 4497–4501.

Fox, H. M. (1932) *Proc. R. Soc. (London) B111*, 356–362.

Fushitani, K., & Riggs, A. F. (1988) *Proc. Natl. Acad. Sci. U.S.A. 85*, 9461–9463.

Geibel, J., Chang, C. K., & Traylor, T. G. (1975) *J. Am. Chem. Soc. 97*, 5924–5926.

Giacometti, G. M., Traylor, T. G., Ascenzi, P., Brunori, M., & Antonini, E. (1977) *J. Biol. Chem. 252*, 7447–7448.

Gibson, Q. H. (1974) *Proc. Natl. Acad. Sci. U.S.A. 70*, 1–4.

Gibson, Q. H. (1989) *J. Biol. Chem. 264*, 20155–20158.

Gibson, Q. H., & Antonini, E. (1967) *J. Biol. Chem. 242*, 4678–4681.

Gibson, Q. H., Bellelli, A., Regan, R., Sharma, P. K., & Vinogradov, S. N. (1992) *J. Biol. Chem. 267*, 11977–11981.

Gill, S. J. (1981) *Methods Enzymol. 76*, 427–438.

Guerritore, D., Bonacci, M. L., Brunori, M., Antonini, E., Wyman, J., & Rossi Fanelli, A. (1965) *J. Mol. Biol. 15*, 88–118.
Henry, E. R., & Hofrichter, J. (1992) *Methods. Enzymol. 210*, 129–140.
Hofrichter, J., Henry, E. R., Szabo, A., Murray, L. P., Ansari, A., Jones, C. M., Coletta, M., Falcioni, G., Brunori, M., & Eaton, W. A. (1991) *Biochemistry 26*, 6583–6592.
Hofrichter, J., Sommer, J. H., Henry, E. R., & Eaton, W. A. (1983) *Proc. Natl. Acad. Sci. U.S.A. 80*, 2235–2239.
Hopfield, J. J., Shulman, R. G., & Ogawa, S. (1971) *J. Mol. Biol. 61*, 425–443.
Huang, Y., Marden, M. C., Lambry, J. C., Fontaine-Aupart, M. P., Pansu, R., Martin, J. L., & Poyart, C. (1991) *J. Am. Chem. Soc. 113*, 9141–9144.
Imai, K. (1973) *Biochemistry 12*, 798–808.
Imai, K. (1981) *Methods Enzymol. 76*, 438–449.
Imai, K., Yoshikawa, S., Fushitani, K., Takizawa, H., Handa, T., & Kirhara, H. (1985) in *Invertebrate oxygen carriers*, pp 367–374, Springer Verlag, Berlin.
Kaminaka, S., Ogura, T., & Kitagawa, T. (1990) *J. Am. Chem. Soc. 112*, 23–27.
Kapp, O. H., Qabar, A. N., Bonner, M. C., Stern, M. S., Walz, D. A., Schmuck, M., Pilz, I., Wall, J. S., & Vinogradov, S. N. (1990) *J. Mol. Biol. 213*, 141–158.
Kuiper, H. A., Antonini, E., & Brunori, M. (1977) *J. Mol. Biol. 116*, 569–576.
Marquardt, D. W. (1963) *J. Soc. Indust. Appl. Math. 11*, 431–441.
Minton, A. P., & Imai, K. (1974) *Proc. Natl. Acad. Sci. U.S.A. 71*, 1418–1421.
Monod, F., Wyman, J., & Changeux, J. P. (1965) *J. Mol. Biol. 15*, 88–118.
Perutz, M. F. (1970) *Nature 228*, 726–734.
Petrich, J. W., Poyart, C., & Martin, J. L. (1989) *Biochemistry 27* 4049–4060.
Qabar, A. N., Stern, M. S., Watz, D. A., Chin, J. T., Timkovich, R., Wall, J. S., Kapp, O. H., & Vinogradov, S. N. (1991) *J. Mol. Biol. 222*, 1109–1129.
Robert, C. H., Decker, H., Richey, B., Gill, S. J., & Wyman, J. (1987) *Proc. Natl. Acad. Sci. U.S.A. 84*, 1891–1895.
Rossi Fanelli, A., & Antonini, E. (1958) *Arch. Biochem. Biophys. 77*, 478–492.
Royer, W. F., Hendrickson, W. A., & Chiancone, E. (1990) *Science 249*, 518–521.
Saffran, W. A., & Gibson, Q. H. (1977) *J. Biol. Chem. 252*, 7955–7958.
Sawiki, C. A., & Gibson, Q. H. (1976) *J. Biol. Chem. 251*, 1533–1542.
Sawiki, C. A., & Gibson, Q. H. (1979) *J. Biol. Chem. 254*, 4058–4062.
Sharma, V. S., Shmidt, M. R., & Ranney, H. N. (1976) *J. Biol. Chem. 251*, 4267–4272.
Su, C., Park, Y. D., Liu, G. Y., & Spiro, T. G. (1989) *J. Am. Chem. Soc. 111*, 3457–3459.
Suzuki, T., & Gotoh, T. (1986) *J. Biol. Chem. 261*, 9257–9267.
van Driel, R., Brunori, M., & Antonini, E. (1974) *J. Mol. Biol. 121*, 431–439.
van Driel, R., Kuiper, H. A., Antonini, E., & Brunori, M. (1978) *J. Mol. Biol. 121*, 431–439.
Vinogradov, S. N., Sharma, P. K., Qabar, A. N., Wall, J. S., Westrick, J. A., Simmons, J. H., & Gill, S. J. (1991) *J. Biol. Chem. 266*, 13091–13096.
Zolla, L., Coletta, M., Di Cera, E., Giardina, B., Kuiper, H., & Brunori, M. (1986) *Biophys. Chem. 24*, 319–325.